Frontiers in Heat and Mass Transfer

Tech Science Press

https://doi.org/10.32604/fhmt.2026.081419

ARTICLE

Experimental Study on the Critical Conditions for Hydrate Formation during CO_2 Driving Oil Recovery

Min Li[1], Haijun Luan[1], Ming Chi[1], Sen Chen[1], Yang Chen[1], Jiarui Cheng[2,*], Tian Xie[2,*] and Rui Wang[2]

[1]Oil Extraction Technology Research Institute, CNPC Xinjiang Oilfield Branch, Karamay, China
[2]School of Mechanical Engineering, Xi'an Shiyou University, Xi'an, China

*Corresponding Authors: Jiarui Cheng. Email: cjr88112@163.com; Tian Xie. Email: xietian@xsyu.edu.cn

Received: 02 March 2026; Accepted: 08 April 2026; Published: 29 June 2026

ABSTRACT: This study used simulated formation water (15 g/L $CaCl_2$) from a certain area of Xinjiang Oilfield as the experimental medium., and employed a high-pressure sealed reaction vessel and a sapphire window to systematically investigate the effects of water content (30%–70%), initial pressure (2–14 MPa), and the intervention of CH_4 on the critical point of CO_2 hydrate formation. The differences between the 'visual confirmation' method and the temperature-pressure curve inflection point method for determining hydrate formation were also compared. The study found that in a single CO_2 system under a constant pressure of 5 MPa and a water content of 30%–70%, no visible hydrate was observed with the naked eye. However, the inflection point method showed that the theoretical critical temperature and pressure increased with the increase in water content. For a 50% water content system, there was a threshold pressure range of 8–11 MPa. Only when the initial pressure was higher than this threshold would visible hydrates form, and the critical point shifted upward with the increase in pressure. In the CO_2-CH_4 mixed system, the critical point under a constant pressure of 10 MPa showed a V-shaped trend with changes in gas ratio, with a minimum point at a 1:1 ratio; the constant ratio and variable pressure experiment indicated that the intervention of CH_4 significantly increased the critical temperature and pressure. Furthermore, the introduction of CH_4 changed the growth position of hydrates, shifting them from the gas-liquid interface to the liquid phase matrix. The study revealed the pressure threshold effect of CO_2 hydrate formation in high mineralization degree formation water systems and the gas component competition mechanism: when the ratio of the two components is balanced, the competitive effect is minimized, forming the optimal formation conditions; as the proportion of CH_4 increases, its competitive advantage strengthens, not only increasing the critical temperature and pressure, but also driving the shift of the hydrate growth position, demonstrating the decisive regulatory role of gas components on the equilibrium and formation kinetics of hydrates, providing experimental basis for the risk prevention of hydrates in the CO_2 flooding process.

KEYWORDS: CO_2 flooding; hydrate formation; water content; pressure

1 Introduction

Under the backdrop of global energy transition and the "dual carbon" strategy, carbon dioxide capture, utilization and storage (CCUS) technology has become a key means for reducing greenhouse gas emissions [1,2]. Among them, carbon dioxide enhanced oil recovery (CO_2-EOR) technology injects CO_2 into oil reservoirs, which can not only increase the oil recovery rate but also achieve geological storage of CO_2, with significant economic and environmental benefits [3,4]. However, during oil extraction, the contact between CO_2 and formation water easily leads to the formation of carbon dioxide hydrates, causing

well blockage and affecting normal production, severely restricting the application and promotion of this technology in various oil reservoirs [5,6].

Natural gas hydrates are crystalline compounds that resemble ice, consisting of a cage-like main framework formed by water molecules through hydrogen bonds, with gas molecules encapsulated within as the guest molecules. Their thermodynamic stability is strictly controlled by temperature and pressure conditions [7,8]. Sloan and Koh systematically expounded the basic thermodynamic and kinetic principles of hydrate formation in their classic work, pointing out that there is a distinct metastable interval in hydrate nucleation, and the nucleation energy barrier varies dynamically with the composition of the system. Only when the overcooling degree of the system exceeds the critical value can the nucleation process occur spontaneously [9,10]. This theory provides a fundamental framework for understanding the behavior of hydrates in complex oil and gas systems.

The water content is a key parameter affecting the formation of hydrates, and its mechanism of action has been systematically studied in pure gas systems. Current research indicates that the activity of water molecules (water activity) and the formation of hydrate nucleation sites may be altered due to the presence of the oil phase [11,12]. Song et al. discovered through emulsion system experiments that when the water content is less than 50%, the system presents an oil-in-water (W/O) type emulsion, and the formation of hydrates has a distinct induction period; while at high water contents (>70%), it transforms into a rapid formation stage [13]. Prasad et al. further pointed out that asphaltenes and resins in crude oil adsorb on the oil-water interface, forming a physical barrier, significantly increasing the nucleation energy barrier of hydrates [14]. However, for complex oil reservoir systems such as the Mahe Oilfield with high salinity and high-water content (30%–70%), the quantitative relationship of the critical conditions for CO_2 hydrate formation has not yet been established.

The accurate determination of the critical point for hydrate formation is the prerequisite for predicting hydrate risks. Current research mainly relies on the "visual observation" method and the inflection point method of temperature-pressure curves [15,16]. Chen et al. found that the visual method consistently provided reliable detection, whereas the pressure drop method failed to clearly identify the onset at lower temperatures. The onset time measured by visual observation was typically shorter than or equal to that determined by the pressure drop method, and the discrepancy between the two methods reflected the inhibiting effect on hydrate crystal growth [16]. Sum et al. pointed out that hydrate nucleation follows the classical nucleation theory (CNT), and the system can remain in an oversaturated state within the metastable zone without undergoing a phase change [10]. Makogon further confirmed that hydrate formation requires the simultaneous satisfaction of thermodynamic undercooling and critical pressure threshold conditions [17]. Ohmura et al. measured the phase equilibrium curve of CO_2 hydrates within the range of 2–10 MPa, confirming the existence of the pressure threshold effect [18].

What is more complex is that the involvement of the associated gas CH_4 during CO_2 oil displacement significantly alters the characteristics of hydrate formation. In the sI type hydrate structure, the CH_4 molecule (with a dynamic diameter of 3.8 Å) can simultaneously occupy the 5^{12} small cage and the $5^{12}6^2$ large cage, while the CO_2 molecule (with a dynamic diameter of 3.3 Å) mainly occupies the $5^{12}6^2$ large cage. The competition for occupation by the two leads to a unique phase equilibrium behavior in the mixed system [19,20]. Ota et al. revealed the cage selectivity mechanism of CH_4 hydrates being replaced by CO_2 through *in-situ* Raman spectroscopy observations, indicating that during the replacement process, CO_2 preferentially occupies the large cage, while CH_4 is enriched in the small cage [21]. Miyatake et al. found that the CH_4-CO_2 mixed gas exhibits "negative azeotropic-like" behavior under specific compositions, that is, the equilibrium point pressure is lower than that of any pure component system, presenting the V-shaped critical curve characteristics [22]. Li et al. [23] employed molecular dynamics simulations to systematically

investigate the dual role of H_2S in promoting nanobubble dissolution and stabilizing specific hydrate cage structures, revealing that H_2S acts as a hydrogen bond donor to repair lattice defects while simultaneously altering cage composition to favor sI hydrate formation. These findings provide fundamental insights into the molecular-level interactions governing sour gas hydrate formation, offering a theoretical basis for developing effective hydrate management strategies in natural gas pipeline systems.

In conclusion, although previous studies have made significant progress in the field of hydrate thermodynamics and kinetics, there are still several key scientific issues that urgently need to be addressed for the special operating conditions of the low-permeability oil reservoirs in the Mahe block under CO_2 flooding: (1) There is a lack of accurate data on the pressure threshold for the formation of CO_2 hydrates within the 30%–70% water content range; (2) The evolution law of the critical point for the formation of hydrates in the CH_4-CO_2 mixed gas in the oil-water coexisting system is still unclear.

In view of this, this study used the simulated formation compatible water from a certain block in Xinjiang Oilfield as the experimental medium, and independently developed a high-pressure visual reaction system. The system investigated the influence laws of water content (30%–70%), initial pressure (2–14 MPa), and gas components (CO_2/CH_4 ratio) on the critical point of hydrate formation. The aim of the study is to reveal the generation mechanism of CO_2 hydrates under the conditions of water content, pressure, and CH_4 intervention, clarify the regulatory laws of CH_4 intervention on the growth morphology and critical conditions of CO_2 hydrates, and provide theoretical support for the optimization of CO_2 drainage process parameters and the prevention of wellbore hydrate blockage.

2 Experimental Section

2.1 Experimental Raw Materials and Operating Conditions Design

The water sample used in the experiment was the simulated formation matching water from a certain block of Xinjiang Oilfield (CaCl2: 15 g/L). The purity of the gases CO_2, CH_4, and Ar used in the experiment was >99.999%. The operating conditions are shown in Table 1.

Table 1: Experimental condition design.

Number	CO_2/%	CH_4/%	Water Content/%	Oil/%	Temperature/°C	Pressure/MPa	Experimental Objective
1	70	—	30	—	0~30	5	Low water content influence
2	50	—	50	—	0~30	5	Reference operating condition
3	30	—	70	—	0~30	5	High water content influence
4~7	50	—	50	—	0~30	2/5/8/11/14	Pressure variation impact
8~18	15~35	15~35	50	—	0~30	10~14	Mixed gas system

2.2 Experimental System

The experimental setup mainly consists of a high-pressure gas supply unit, a visual reaction unit, and a data acquisition unit. The physical and schematic representation of the system is shown in Fig. 1. The core equipment is a 100 mL visual reaction vessel with a 316L stainless steel body, capable of withstanding a maximum pressure of 30 MPa and a maximum temperature of 150°C. A 4 cm diameter sapphire window is provided for real-time observation. Temperature control is achieved through a high-low temperature thermostat (−20°C~150°C, with an accuracy of ±0.1°C), and the cooling rate is 0.5°C/min, while the heating rate is 2°C/min. Pressure and temperature are monitored using 0.25-class pressure sensors (0~20 MPa) and PT100 thermoresistors (with an accuracy of ±0.4%), and the data sampling frequency is 1 Hz.

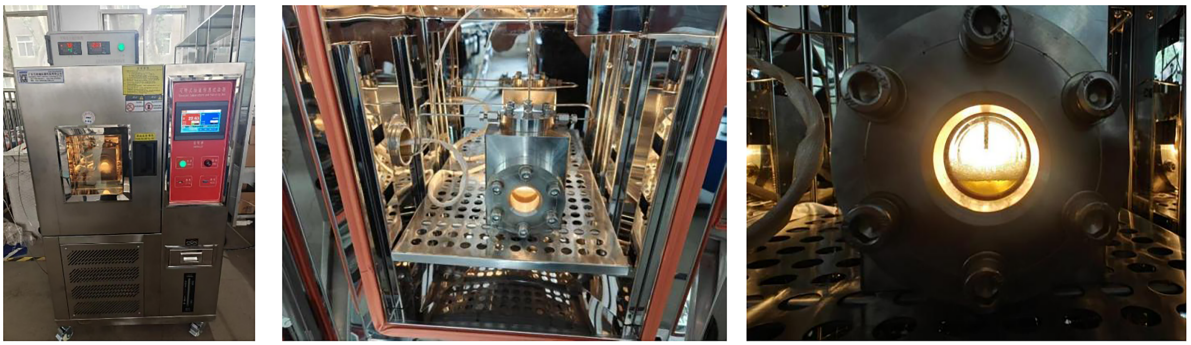

Figure 1: Physical diagram of the experimental system.

2.3 Experimental Procedures

Step 1: Based on the design calculation values, quantitatively add formation water to the reaction vessel (error < ±0.5 mL);

Step 2: Introduce argon gas for three purging cycles to remove air, then increase the pressure to 2 MPa for leak detection. Confirm the sealing performance and then depressurize to normal pressure;

Step 3: Through the gas pressurization system, inject the designed working condition gas into the vessel to reach the target pressure (error ±0.05 MPa);

Step 4: Start the temperature control program, cool down at a rate of 0.5°C/min to 0°C. Continuously observe through the sapphire window and simultaneously record temperature and pressure data;

Step 5: After identifying the critical point of hydrate formation, continue to cool down to 1°C or observe until the crystal growth stabilizes.

3 Results

3.1 Influence of Water Content

The effect of water content ranging from 30% to 70% on the critical point of CO_2 hydrate formation was investigated under a constant pressure of 5 MPa. The entire experiment was observed through a sapphire window, as shown in Figs. 2–4. The temperature-pressure change curves during the cooling process under different water content conditions are presented in Fig. 5. It is necessary to note that, based on previous research results, there are generally two methods for determining the critical point of hydrate formation: the "seeing is believing" method, which is the temperature and pressure corresponding to the visible formation of hydrates with the naked eye, and the theoretical determination method, which is based on the sudden

change points in the temperature-pressure curve, such as the sudden drop in pressure during the cooling process or the sudden rise in pressure during the heating process, and is considered as the critical state point of hydrate formation [15,16]. Of course, both methods for determining hydrate formation follow their own rules, and for the same influencing factor, they are not suitable for mixed use. As can be seen from Figs. 2–4, when the visible formation of hydrates is used as the determination basis, with the pressure controlled at 5 MPa and the temperature decreased from 25°C to 2°C, no hydrates will form in the water-vapor system regardless of the water content ranging from 30% to 70%.

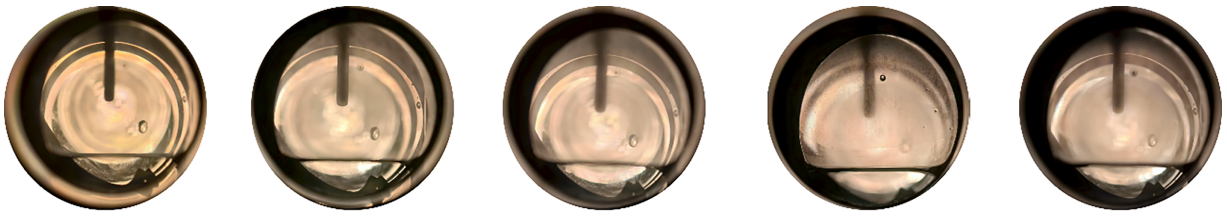

Figure 2: Observation diagram of the experimental process at 30% water content + single CO_2 (P = 5 MPa).

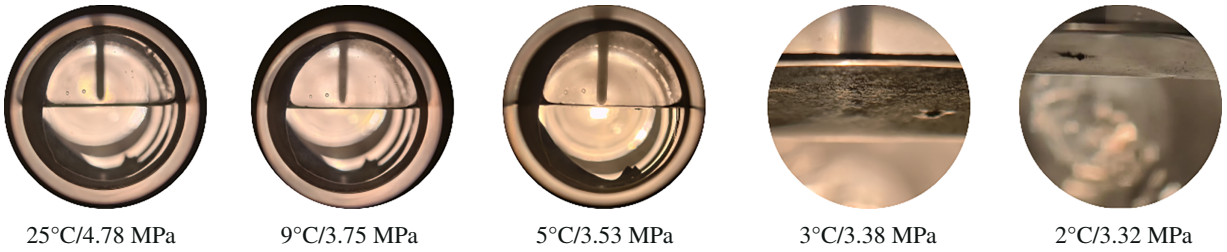

Figure 3: Observation diagram of the experimental process at 50% water content + single CO_2 (P = 5 MPa).

Figure 4: Observation diagram of the experimental process at 70% water content + single CO_2 (P = 5 MPa).

When the inflection point method is used as the criterion for detecting pre-nucleation phenomena, distinct behaviors were observed across different water content conditions. For the 70% water content condition, a slight fluctuation appeared in the pressure curve at 13.5°C/4.27 MPa. This is attributed to the formation of local "water cluster structures" by excess water molecules, which temporarily adsorb CO_2 molecules and cause a slight increase in the gas consumption rate. However, this adsorption is unstable and does not trigger actual nucleation. For the 50% water content condition, no visible hydrate crystals were observed, yet a significant inflection point occurred at 9°C/3.75 MPa. This temperature is close to the metastable zone of CO_2 hydrate, where CO_2 and water molecules form transient "quasi-hydrate structures." Hydrogen bonding between these molecules alters the system's compressibility, but due to insufficient

energy to overcome the nucleation barrier, these structures do not develop into stable nuclei. For the 30% water content condition, the system remained in a transparent gas-liquid two-phase state throughout the experiment, with no white crystals, flocs, or turbidity observed. The pressure decreased smoothly from 4.91 MPa at 25°C to 3.71 MPa at 3°C, exhibiting a nearly perfect linear relationship, indicating that only physical cooling occurred without any hydrate-related phenomena.

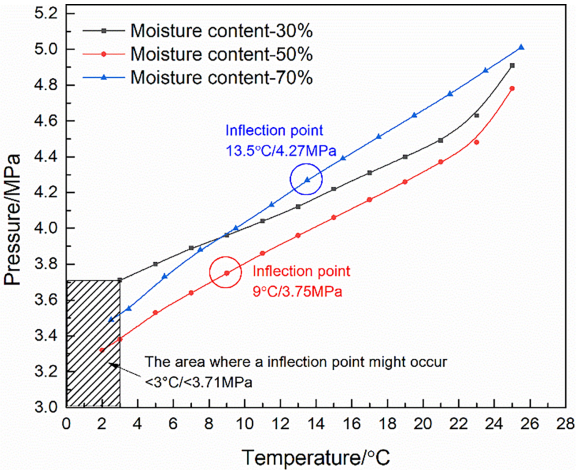

Figure 5: The influence of different water contents on the formation of CO_2 hydrates.

Importantly, these inflection points reflect the conditions for transient cluster formation and pre-nucleation molecular rearrangements, not the formation of stable, macroscopic hydrates. Based on the absence of both visual confirmation and inflection points under the 30% water content condition, it can be inferred that if hydrate formation were to occur, the critical conditions would likely require a temperature lower than 3°C and a pressure lower than 3.71 MPa. In summary, the inflection point method reveals a trend in the pre-nucleation regime: as water content increases, the temperature and pressure conditions required for the onset of transient molecular clustering and quasi-hydrate structures gradually increase. However, these conditions should not be equated with the critical temperature and pressure for stable hydrate formation, which require visual confirmation of crystalline hydrates.

3.2 Impact of Pressure

At a water content of 50%, the influence of pressure (2–14 MPa) on the evolution characteristics of the critical point of CO_2 hydrate formation was investigated. The experimental process is shown in Figs. 6–9. The temperature-pressure variation curves during the cooling process under different pressure conditions are shown in Fig. 10. From Figs. 3 and 6–9, it can be seen that when the temperature gradually decreases, hydrate does not form in the low-pressure zone (2–8 MPa). In the high-pressure zone (11 and 14 MPa), hydrate crystals grow at the liquid surface. Under the 11 MPa condition, the critical temperature for the appearance of visible hydrate is 2°C, and the critical pressure is 3.75 MPa. Under the 14 MPa condition, the critical point of hydrate formation shifts upward to 3°C/3.88 MPa. It is worth noting here that the formation of hydrate crystals initially occurs mainly at the gas-liquid interface position, and then gradually expands towards the liquid phase region and the gas phase region. Of course, the point we are most concerned about is still the relationship between the initial pressure and the critical point for hydrate formation. When using the visible hydrate formation method as the judgment criterion, when the water content is kept constant at 50% and the temperature is reduced from 25°C to 1°C, only when the initial pressure of the water-gas

system reaches the 8 MPa condition will hydrate possibly form. When the initial pressure is below 8 MPa, no hydrate will be formed. Moreover, the critical temperature and critical pressure for hydrate formation show a gradually increasing trend as the initial pressure condition increases. In summary, under the condition of 50% water content, there is a threshold pressure for the formation of CO_2 hydrates. This threshold pressure is between 8 and 11 MPa. Only when the initial pressure is higher than this threshold pressure can CO_2 hydrates possibly form.

Figure 6: Observation diagram of the experimental process at 50% water content + single CO_2 (P = 2 MPa).

Figure 7: Observation diagram of the experimental process at 50% water content + single CO_2 (P = 8 MPa).

Figure 8: Observation diagram of the experimental process at 50% water content + single CO_2 (P = 11 MPa).

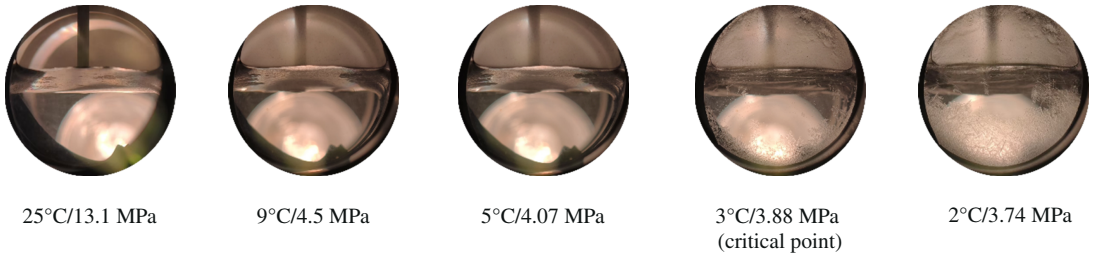

Figure 9: Observation diagram of the experimental process at 50% water content + single CO_2 (P = 14 MPa).

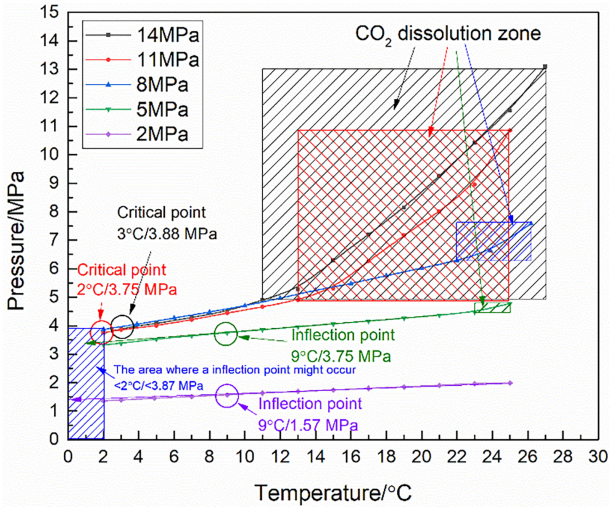

Figure 10: The influence of different pressures on the formation of CO_2 hydrates (50% water content + single CO_2 system).

3.3 CO_2 + CH_4 Mixture Gas System

3.3.1 Adjusting Gas Ratio While Keeping the Total Pressure Constant (10 MPa)

Under the conditions of a water content of 50% and a constant pressure of 10 MPa, the influence of the composition of gas components on the evolution characteristics of the critical point for the formation of CO_2 hydrates was investigated. This is because for the production wells in the CO_2 drainage process, the main components of the associated gas are CH_4 and CO_2. The experimental process is shown in Figs. 11–13. The temperature-pressure variation curves during the cooling process under different gas component conditions are shown in Fig. 14. From Figs. 11–13, it can be seen that when the reaction system maintains a pressure of 10 MPa, the proportion of the transformed gas phase composition will result in the formation of hydrates. When the ratio of CO_2 to CH_4 in the gas phase is 3:7, the critical point for the formation of hydrates is 4°C/6.85 MPa. When the ratio of CO_2 to CH_4 in the gas phase is 1:1, the critical point for the formation of hydrates is 5°C/5.86 MPa. When the ratio of CO_2 to CH_4 in the gas phase is 7:3, the critical point for the formation of hydrates is 10°C/7.95 MPa. From Fig. 14, it can be observed that the variation of the critical point for hydrate formation follows a V-shaped trend. Based on the ratio of CO_2 to CH_4 in the gas phase being 1:1 as the reference, when the proportion of methane in the gas phase increases, the critical temperature for hydrate formation will gradually decrease, while the critical pressure will gradually increase; when the proportion of carbon dioxide in the gas phase increases, the critical temperature for hydrate formation will gradually increase, while the critical pressure will gradually decrease. Moreover, unlike the case where there is only a single CO_2 in the gas phase composition, when methane is involved in the gas, hydrate is preferentially produced from the liquid phase. As the temperature drops, the hydrate gradually breaks through the gas-liquid interface and grows into the gas phase. In summary, the intervention of CH_4 has a certain impact on the critical point and growth morphology of CO_2 hydrates. When the proportion of methane in the gas phase is dominant, the continuous increase of the methane proportion will cause an abnormal increase in the critical pressure for hydrate formation.

Figure 11: Observation diagram of the experimental process at 50% water content + mixed gas (CO_2-15% + CH_4-35%).

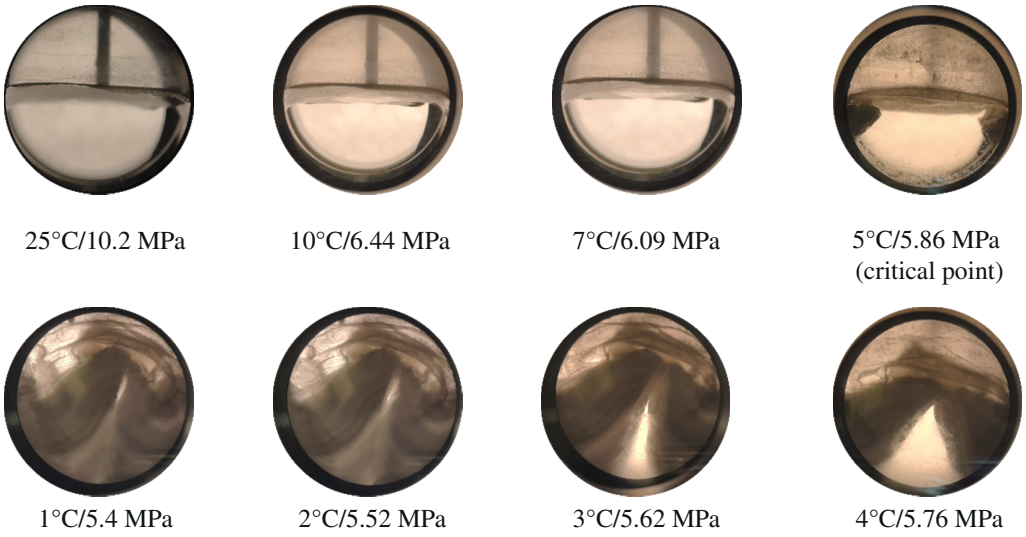

Figure 12: Observation diagram of the experimental process at 50% water content + mixed gas (CO_2-25% + CH_4-25%).

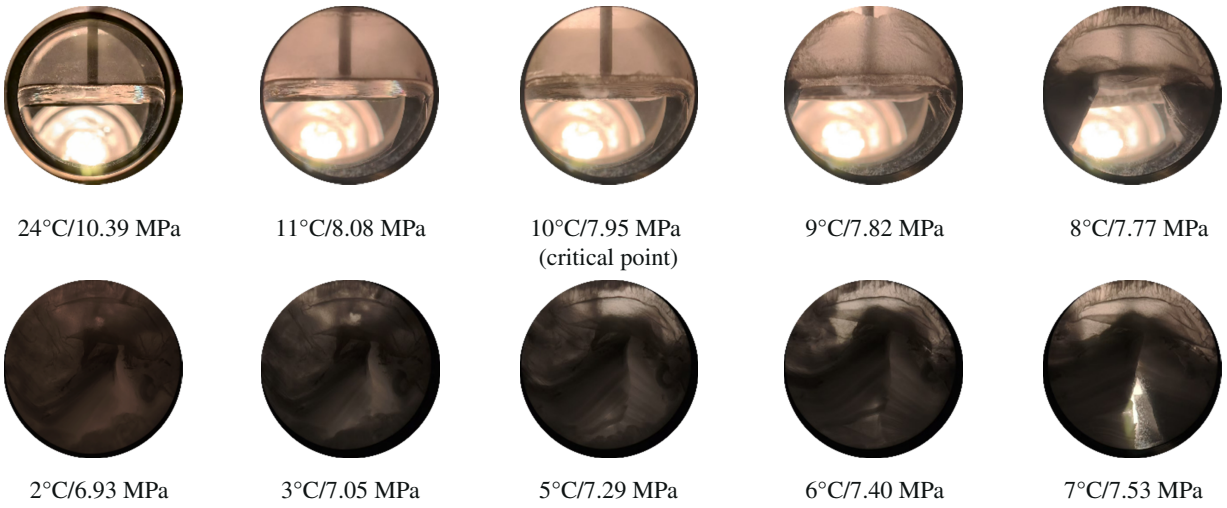

Figure 13: Observation diagram of the experimental process at 50% water content + mixed gas (CO_2-35% + CH_4-15%).

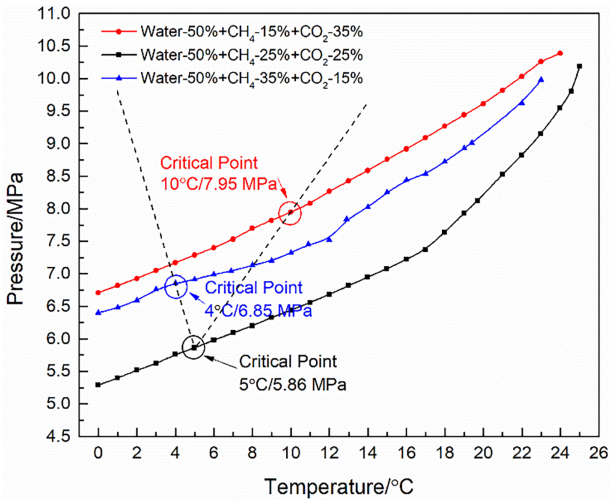

Figure 14: The influence of the proportion of gas components in the mixture on the critical point for hydrate formation.

3.3.2 Proportional Change (1:1) in Total Pressure

Under the conditions of a water content of 50% and a fixed composition ratio of gas components, the influence of gas pressure (ranging from 10 to 14 MPa) on the critical point of CO_2 hydrate formation was investigated. The experimental process is shown in Figs. 15 and 16. The temperature-pressure variation curves during the cooling process under different pressure conditions are shown in Fig. 17. From Figs. 15 and 16, it can be seen that when the proportion of gas components in the reaction system remains unchanged, changes in pressure will result in visible hydrate formation. At a pressure of 10 MPa, the critical point for hydrate formation is 5°C/5.86 MPa; at 12 MPa, the critical point is 10°C/8.24 MPa; and at 14 MPa, the critical point is 11°C/9.71 MPa. As the initial pressure increases, the critical temperature and critical pressure for hydrate formation also gradually increase, which is similar to the trend of single CO_2 hydrate formation with pressure. This is because the increase in total pressure increases the number density of gas molecules and the collision

frequency. Compared with the single CO_2 condition, the intervention of CH_4 has greatly increased the critical temperature and critical pressure for hydrate formation.

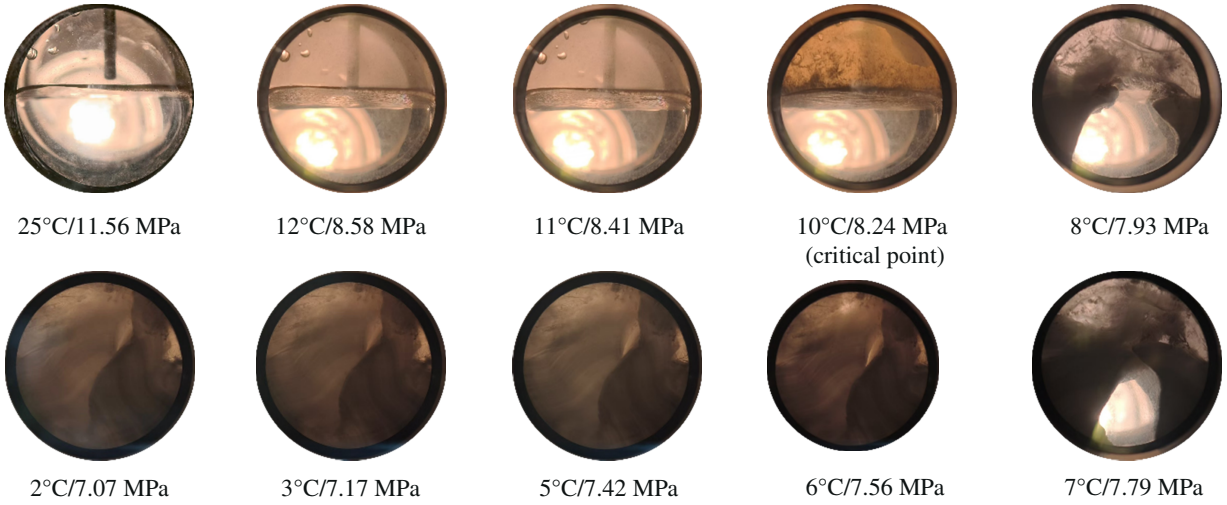

Figure 15: The influence of varying total pressure to 12 MPa on the 1:1 mixed system.

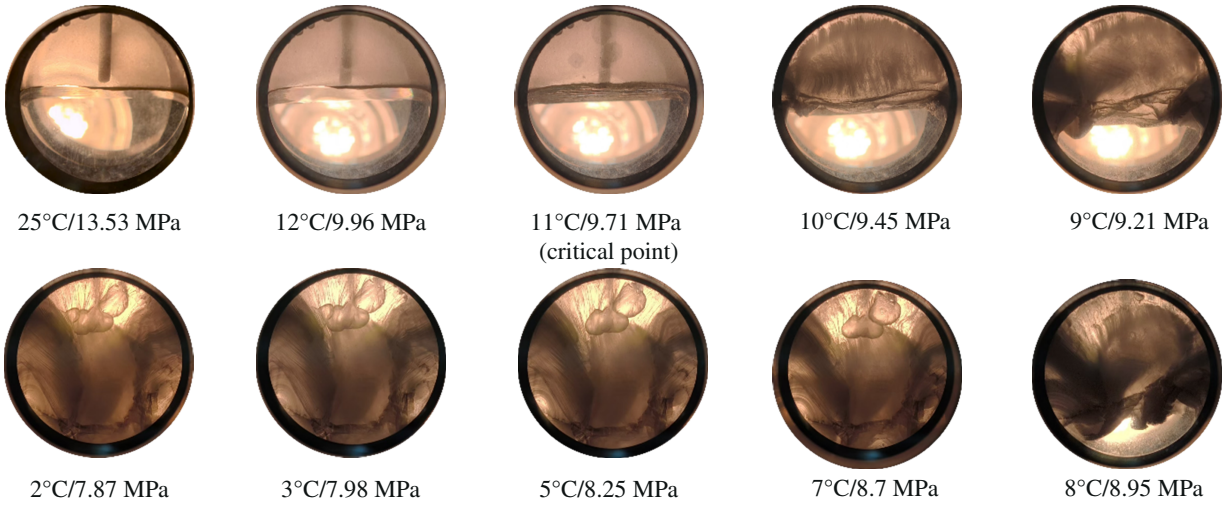

Figure 16: The influence of varying total pressure to 14 MPa on the 1:1 mixed system.

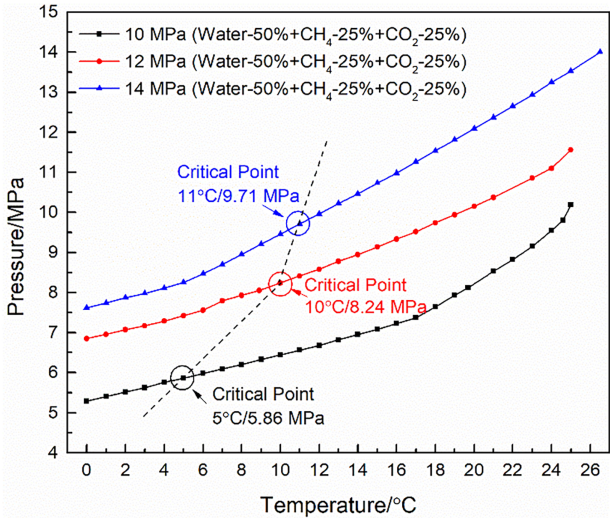

Figure 17: The influence of mixed gas pressure on the critical point for hydrate formation.

4 Discussion

4.1 Mechanism of the Influence of Water Content and Pressure Threshold under Pure CO_2 Conditions

This study found that under a constant pressure of 5 MPa, no visible CO_2 hydrate was formed within the water content range of 30% to 70%. This result differs from the rapid formation stage reported by Song et al. [13] at high water contents (>70%). It reveals the regulatory effect of pressure conditions on the water content effect. According to the metastable theory proposed by Christiansen et al. [9,10], hydrate nucleation requires a critical supercooling degree to overcome the nucleation energy barrier. In this experiment, the temperature-pressure trajectories of each water content system at 5 MPa were all on the left side of the metastable zone and did not reach the critical driving force required for nucleation. As the water content increased from 30% to 70%, the critical temperature and pressure detected by the turning point method showed an upward trend, which is consistent with the mechanism proposed by Prasad et al. [14] regarding the shift of phase equilibrium conditions towards lower temperatures and higher pressures due to the decrease in water activity. In high water content systems, excess water molecules form local "water cluster structures" (water clusters), which can temporarily adsorb CO_2 molecules (such as at 13.5°C with a pressure fluctuation at 70% water content). However, due to the insufficient stability of the hydrogen bond network between molecules, they failed to form stable critical nuclei [24].

It is particularly important that this study has for the first time identified a pressure threshold effect of 8–11 MPa in the formation water system of the Mahe block. Ohmura et al. [18] measured the pressure threshold for CO_2 hydrate formation in a pure water system to be approximately 2.5–3.0 MPa (in the 0°C–10°C range), while in this study, when the water content was 50%, it was found that when the initial pressure was lower than 8 MPa, even when the temperature dropped to 1°C, no hydrate formation was observed. This indicates that the actual formation fluid system (containing salinity and organic matter) significantly raises the pressure threshold required for nucleation. This difference stems from the inhibition of water activity by the ionic strength of the formation water and the adsorption of dissolved organic matter at the gas-liquid interface, effectively increasing the nucleation barrier [14,25]. When the pressure exceeded 11 MPa, the critical temperature increased positively with the initial pressure, which conforms to the gas-liquid two-phase equilibrium law described by the Clapeyron equation [26]. However, the slope was more gentle

than that of the pure water system, suggesting that the change in gas solubility in the formation compatible water system has a buffering effect on the phase equilibrium.

4.2 Complementarity of Visual Observation and the Turning Point Method

This study compared the "visual confirmation" method and the inflection point method as two critical judgment criteria, and found that they exhibited systematic differences in the saline formation water system. Chen et al. [16] pointed out that the inflection point method determines the critical state by monitoring pressure sudden drop or the distortion point of the temperature-pressure curve, which is usually lagging behind visual observation; however, this study found that at the water content conditions of 50% and 70%, the inflection point method detected sub-stable signals at 9°C and 13.5°C, respectively, while visual observation never showed white crystals. This contradictory phenomenon can be explained as follows: Firstly, the mineral salts (NaCl, $CaCl_2$, etc.) in the formation water change the ionic strength of the solution, inhibiting the macroscopic growth rate of hydrate crystals, resulting in the initial stage of crystal nuclei being in a nanoscale dispersed state and unable to form visible turbidity or crystallization [1,26]; Secondly, the inflection point method captures the sudden change in the compressibility of the system, corresponding to the reorganization of the hydrogen bond network when CO_2 molecules and water molecules form a transient "quasi-hydrate structure" [9], and this signal occurs before the macroscopic phase change. Therefore, in engineering practice, it is recommended to use the inflection point method as an early warning indicator, while visual observation is used to verify the risk of complete blockage.

4.3 Competitive Mechanism of the CO_2-CH_4 Mixture System

In this study, under a constant pressure of 10 MPa, it was found that the critical point for the formation of hydrates of the CO_2-CH_4 mixed gas varies in a V-shaped curve with the change of gas proportions. This reaches its lowest point at CO_2:CH_4 = 1:1 (5°C/5.86 MPa), which is highly consistent with the "negative azeotropic-like" behavior reported by Miyatake et al. [22]. From the perspective of cage occupancy, this V-shaped curve results from the competition and synergy between the two gas molecules for the sI-type hydrate cage structure [19,21]: when the proportion of CO_2 is too high (70%), although it is conducive to the stable occupation of large cages ($5^{12}6^2$), the insufficient filling of small cages (5^{12}) leads to an increase in lattice defects, resulting in an increase in the critical temperature; when the proportion of CH_4 is too high (70%), the disorder competition of CH_4 molecules (with a dynamic diameter of 3.8 Å) between large and small cages causes an increase in lattice tension, while the decrease in CO_2 partial pressure in the gas phase leads to a decrease in the occupancy rate of large cages, and both of these jointly cause an abnormal increase in the critical pressure [20]. Ota et al. [21] confirmed through Raman spectroscopy that there is a significant cage selectivity during the CO_2-CH_4 substitution process, with CO_2 preferentially occupying large cages and CH_4 being enriched in small cages. The lowest point of the V-shaped curve in this study precisely corresponds to the optimal coexistence ratio of the two gases in cage occupancy, at which the filling rates of large and small cages reach the optimal match, and the Gibbs free energy of the system is at its minimum [22].

It is worth noting that when the proportion of the gas component methane exceeds 15%, the location of hydrate formation shifts from the gas-liquid interface in the case of pure CO_2 to the liquid phase itself. As shown in Fig. 18. This morphological transformation mechanism is closely related to the high solubility of CH_4 in the aqueous phase (compared to CO_2): high concentration of CH_4 dissolution forms a local supersaturated zone, reducing the heterogeneous nucleation energy barrier in the liquid phase. Moreover, the involvement of CH_4 significantly enhances the critical temperature (compared to 11 MPa for pure CO_2, where the critical temperature for CO_2 hydrate formation is 2°C, while the 1:1 mixture of CO_2-CH_4 has reached 5°C at 10 MPa), which is consistent with the phenomenon observed by Sun et al. that CH_4 promotes

the formation of CO_2 hydrates, attributed to CH_4's stabilizing effect on the hydrate lattice as an auxiliary guest [27].

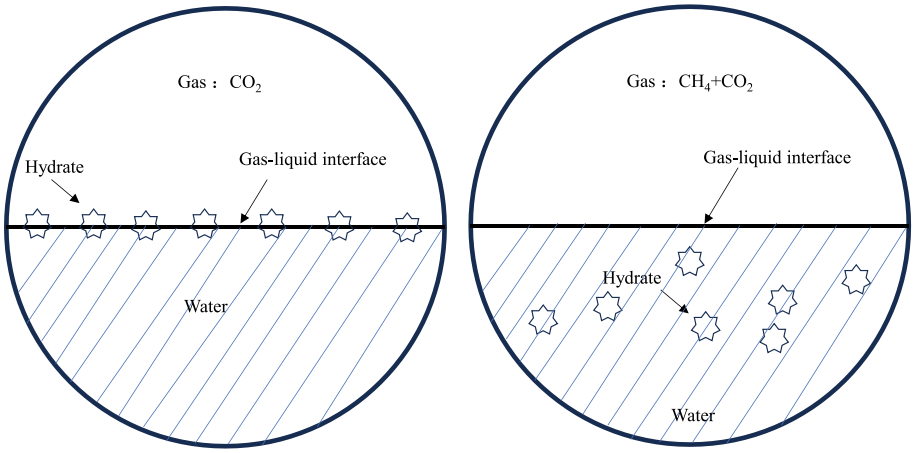

Figure 18: Diagram of hydrate formation.

A significant morphological transformation occurs when the proportion of CH_4 in the gas phase exceeds 50%: the hydrate nucleation and growth location shifts from the gas-liquid interface (characteristic of pure CO_2 systems) to the bulk liquid phase itself. This shift is mechanistically driven by the markedly higher solubility of CH_4 in water compared to CO_2. Under the experimental pressure of 10 MPa, CH_4 dissolves into the aqueous phase at concentrations substantially exceeding those of CO_2, creating localized zones of supersaturation within the bulk liquid. These supersaturated regions effectively lower the heterogeneous nucleation energy barrier in the liquid phase, as the increased chemical potential of dissolved CH_4 molecules reduces the thermodynamic driving force required for critical nucleus formation. Consequently, nucleation is no longer confined to the interface where gas molecules must first cross the phase boundary; instead, it becomes favorable throughout the liquid volume where dissolved CH_4 concentration is highest.

This mechanism contrasts sharply with pure CO_2 systems, where the relatively lower solubility of CO_2 necessitates direct contact between the gas phase and water at the interface for sufficient molecular availability to initiate nucleation. The transition from interface-dominated to bulk-dominated nucleation represents a fundamental change in the kinetic pathway of hydrate formation, with implications for growth rate, crystal morphology, and mass transfer limitations. Furthermore, the involvement of CH_4 significantly elevates the critical temperature compared to pure CO_2 systems: while pure CO_2 requires 11 MPa to achieve a critical temperature of 2°C, the equimolar CO_2-CH_4 mixture reaches 5°C at only 10 MPa. This promotional effect is consistent with Sun et al.'s observation that CH_4 acts as an auxiliary guest, stabilizing the hydrate lattice through optimized cage filling and enhanced thermodynamic stability [27].

5 Conclusion

This paper uses the simulated formation fluid of a certain block in Xinjiang Oilfield as the medium, and employs a high-pressure sealed reaction vessel combined with a sapphire window to systematically investigate the effects of water content (30%–70%), initial pressure (2–14 MPa), and gas components on the critical point of CO_2 hydrate formation. The following conclusions are drawn.

(1) Under pure CO_2 conditions, at an initial pressure of 5 MPa and a temperature drop to 2°C, no visible hydrate formation was observed within the water content range of 30% to 70%. The inflection point of the temperature-pressure curve method indicated that as the water content increased from 30% to

70%, the theoretical critical temperature and pressure for hydrate formation gradually increased. There was an initial pressure threshold of 8 to 11 MPa for visible hydrate formation at a water content of 50%. Only when the initial pressure was higher than this threshold (11 and 14 MPa conditions), could hydrate crystals be observed at the gas-liquid interface, and the critical point shifted upward with the increase in initial pressure (11 MPa: 2°C/3.75 MPa; 14 MPa: 3.8°C/3.99 MPa); when the initial pressure was lower than 8 MPa, no hydrate formation occurred even when the temperature dropped to 1°C.

(2) Under the conditions of CO_2-CH_4, at a total pressure of 10 MPa and a water content of 50%, the hydrate formation critical point of the CO_2-CH_4 mixed gas shows a V-shaped trend with the change of gas ratio. The lowest point occurs when the ratio of CO_2 to CH_4 is 1:1 (5°C/5.86 MPa). When the proportion of CH_4 is dominant (>50%), the critical pressure abnormally increases, and the growth position of the hydrate shifts from the gas-liquid interface of the single CO_2 system to the liquid phase matrix. Under the conditions of CO_2:CH_4 = 1:1 and a water content of 50%, the intervention of CH_4 significantly enhances the critical temperature and pressure for hydrate formation (compared to the single CO_2 system). Within the range of 10 to 14 MPa, the critical point of hydrate formation increases with the increase of total pressure (10 MPa: 5°C/5.86 MPa; 14 MPa: 11°C/9.71 MPa).

Acknowledgement: Not applicable.

Funding Statement: This research was funded by Experimental and Scaling-up Study on Efficient Development of Tight Conglomerate Reservoirs Using CO_2 Miscible Drive in the National Science and Technology Major Project of China (grant No. 2025ZD1408405).

Author Contributions: The authors confirm contribution to the paper as follows: study conception and design: Jiarui Cheng, Tian Xie; data collection: Min Li, Haijun Luan, Ming Chi, Sen Chen, Yang Chen, Jiarui Cheng; analysis and interpretation of results: Rui Wang, Jiarui Cheng, Tian Xie; draft manuscript preparation: Min Li, Jiarui Cheng, Tian Xie. All authors reviewed and approved the final version of the manuscript.

Availability of Data and Materials: Data not available due to commercial restrictions. Due to the nature of this research, participants of this study did not agree for their data to be shared publicly, so supporting data is not available.

Ethics Approval: Not applicable.

Conflicts of Interest: The authors declare no conflicts of interest.

References

1. Zha L, Liang DQ, Li DL. Phase equilibria of CO_2 hydrate in NaCl-$MgCl_2$ aqueous solutions. J Chem Thermodyn. 2012;55:110–4. doi:10.1016/j.jct.2012.06.025.
2. Aghajanloo M, Yan L, Berg S, Voskov D, Farajzadeh R. Impact of CO_2 hydrates on injectivity during CO_2 storage in depleted gas fields: a literature review. Gas Sci Eng. 2024;123(4):205250. doi:10.1016/j.jgsce.2024.205250.
3. Prasad SK, Sangwai JS, Byun HS. A review of the supercritical CO_2 fluid applications for improved oil and gas production and associated carbon storage. J CO_2 Util. 2023;72:102479. doi:10.1016/j.jcou.2023.102479.
4. Chen J, Zeng Y, Liu C, Kang M, Chen G, Deng B, et al. Methane hydrate dissociation from anti-agglomerants containing oil dominated dispersed systems. Fuel. 2021;294:120561. doi:10.1016/j.fuel.2021.120561.
5. Sloan ED Jr, Koh CA, Koh CA. Clathrate hydrates of natural gases. 3rd ed. Boca Raton, FL, USA: CRC Press; 2007. doi:10.1201/9781420008494.
6. Li S, Fan S, Wang J, Lang X, Liang D. CO_2 capture from binary mixture via forming hydrate with the help of tetra-n-butyl ammonium bromide. J Nat Gas Chem. 2009;18(1):15–20. doi:10.1016/S1003-9953(08)60085-7.
7. Makogon YF. Natural gas hydrates-a promising source of energy. J Nat Gas Sci Eng. 2010;2(1):49–59. doi:10.1016/j.jngse.2009.12.004.

8. Koh CA, Sum AK, Sloan ED. Gas hydrates: unlocking the energy from icy cages. J Appl Phys. 2009;106(6):061101. doi:10.1063/1.3216463.
9. Christiansen RL, Sloan ED JR. Mechanisms and kinetics of hydrate formation. Ann N Y Acad Sci. 1994;715(1):283–305. doi:10.1111/j.1749-6632.1994.tb38841.x.
10. Sum AK, Koh CA, Sloan ED. Clathrate hydrates: from laboratory science to engineering practice. Ind Eng Chem Res. 2009;48(16):7457–65. doi:10.1021/ie900679m.
11. Xiang CS, Peng BZ, Liu H, Sun CY, Chen GJ, Sun BJ. Hydrate formation/dissociation in (natural gas + water + diesel oil) emulsion systems. Energies. 2013;6(2):1009–22. doi:10.3390/en6021009.
12. Lv YN, Jia ML, Chen J, Sun CY, Gong J, Chen GJ, et al. Self-preservation effect for hydrate dissociation in water + diesel oil dispersion systems. Energy Fuels. 2015;29(9):5563–72. doi:10.1021/acs.energyfuels.5b00837.
13. Song G, Li Y, Wang W, Jiang K, Shi Z, Yao S. Hydrate formation in oil-water systems: investigations of the influences of water cut and anti-agglomerant. Chin J Chem Eng. 2020;28(2):369–77. doi:10.1016/j.cjche.2019.07.024.
14. Prasad SK, Nair VC, Sangwai JS. Effect of asphaltenes on the kinetics of methane hydrate formation and dissociation in oil-in-water dispersion systems containing light saturated and aromatic hydrocarbons. Energy Fuels. 2021;35(21):17410–23. doi:10.1021/acs.energyfuels.1c02252.
15. Abbasi A, Hashim FM. A review on fundamental principles of a natural gas hydrate formation prediction. Petrol Sci Technol. 2022;40(19):2382–404. doi:10.1080/10916466.2022.2042559.
16. Chen LT, Sun CY, Chen GJ, Zuo JY, Ng HJ. Assessment of hydrate kinetic inhibitors with visual observations. Fluid Phase Equilib. 2010;298(1):143–9. doi:10.1016/j.fluid.2010.07.024.
17. Makogon TY. Handbook of multiphase flow assurance. Amsterdam, The Netherlands: Elsevier Science & Technology; 2019.
18. Ohmura R, Kashiwazaki S, Shiota S, Tsuji H, Mori YH. Structure-I and structure-H hydrate formation using water spraying. Energy Fuels. 2002;16(5):1141–7. doi:10.1021/ef0200727.
19. Veluswamy HP, Wong AJH, Babu P, Kumar R, Kulprathipanja S, Rangsunvigit P, et al. Rapid methane hydrate formation to develop a cost effective large scale energy storage system. Chem Eng J. 2016;290:161–73. doi:10.1016/j.cej.2016.01.026.
20. Koyama Y, Tanaka H, Koga K. On the thermodynamic stability and structural transition of clathrate hydrates. J Chem Phys. 2005;122(7):074503. doi:10.1063/1.1850904.
21. Ota M, Saito T, Aida T, Watanabe M, Sato Y, Smith RL Jr, et al. Macro and microscopic CH_4–CO_2 replacement in CH_4 hydrate under pressurized CO_2. AlChE J. 2007;53(10):2715–21. doi:10.1002/aic.11294.
22. Miyatake R, Sugahara T, Ishikawa T, Oshima M, Jin Y, Hirai T. Isothermal phase equilibria of the CH_4+CO_2 mixed-gas hydrate system for CO_2 capture and storage in a reservoir after CH_4 hydrate exploitation. J Chem Eng Data. 2024;69(9):3210–6.
23. Li Z, Yu W, Ding L, Mi Y, Chen Y, Chen N, et al. Unraveling the microscopic influence mechanism of H_2S on methane hydrate formation via molecular simulation techniques. Langmuir. 2026;42(1):860–72. doi:10.1021/acs.langmuir.5c04991.
24. Uchida T, Yamazaki K, Gohara K. Generation of micro- and nano-bubbles in water by dissociation of gas hydrates. Korean J Chem Eng. 2016;33(5):1749–55. doi:10.1007/s11814-016-0032-7.
25. Dong S, Li M, Firoozabadi A. Effect of salt and water cuts on hydrate anti-agglomeration in a gas condensate system at high pressure. Fuel. 2017;210:713–20. doi:10.1016/j.fuel.2017.08.096.
26. Li X, Fan S, Wang Y, Li G, Wang S, Lang X, et al. Hydrate phase equilibrium of hydrogen-natural gas blends: experimental study and thermodynamic modeling. Fluid Phase Equilib. 2022;556:113417. doi:10.1016/j.fluid.2022.113417.
27. Sun YH, Li SL, Zhang GB, Guo W, Zhu YH. Hydrate phase equilibrium of CH_4+N_2+CO_2 gas mixtures and cage occupancy behaviors. Ind Eng Chem Res. 2017;56(28):8133–42. doi:10.1021/acs.iecr.7b01093.